ELSEVIER

Microelectronic Engineering 1 (2002) 000–000

MICROELECTRONIC ENGINEERING

www.elsevier.com/locate/mee

Single-electron control of Wigner crystallization

M. Bonitz[a,*], V Golubnychiy[a], A.V. Filinov[a,b], Yu.E. Lozovik[b]

[a]*Universitat Rostock, Fachbereich Physik, Universitatsplatz 3, D-18051 Rostock, Germany*
[b]*Institute of Spectroscopy, 142090 Troitsk, Russia*

Abstract

Wigner crystallization in mesoscopic quantum dots containing only few ($N < 50$) electrons exhibits a number of interesting peculiarities: (i) there exist two distinct crystal phases, and (ii) the phase boundary sensitively depends on the precise particle number. In this paper we demonstrate that this behavior can be used to control the *collective* transport properties by adding or removing a *single electron*. © 2002 Published by Elsevier Science B.V.

Keywords: Wigner crystal; Quantum dot; Mesoscopic systems; Metal–insulator transition

One of the most exciting properties of mesoscopic systems is the dependence of their properties on the particle number. Besides the familiar electron addition spectra in quantum dots, e.g. Ref. [1] recently, another example has been found, cf. Refs. [2,3] and references therein: Wigner crystallization in mesoscopic electron clusters in two-dimensional quantum dots. Simulations of a small number of electrons confined in a spherically symmetric harmonic trap and interacting via the Coulomb potential [3,4] revealed that the location of the phase boundary of the Wigner crystal in the density–temperature plane sensitively depends on the precise particle number. In this paper we discuss principle possibilities of taking advantage of this behavior for applications.

The particle number sensitivity originates from the configuration symmetry of the cluster ground state. Minimization of the total energy computed from the Hamiltonian

$$\hat{H} = -\sum_{i=1}^{N} \frac{\hbar^2 \nabla_i^2}{2m_i^*} + \sum_{i=1}^{N} \frac{m_i^* \omega_0^2 r_i^2}{2} + \sum_{i<j}^{N} \frac{e^2}{\epsilon_b |\mathbf{r}_i - \mathbf{r}_j|}, \tag{1}$$

(m^* and ϵ_b are the effective electron mass and background dielectric constant, respectively), yields a spherical shell structure details of which vary strongly with the particle number, see Fig. 1. 'Magic' clusters (those with an integer ratio of particle numbers on the outer and inner shell—e.g. $N = 19$)

*Corresponding author.
E-mail address: michael.bonitz@physik.uni-rostock.de (M. Bonitz).

0167-9317/02/$ – see front matter
PII: S0167-9317(02)00624-X

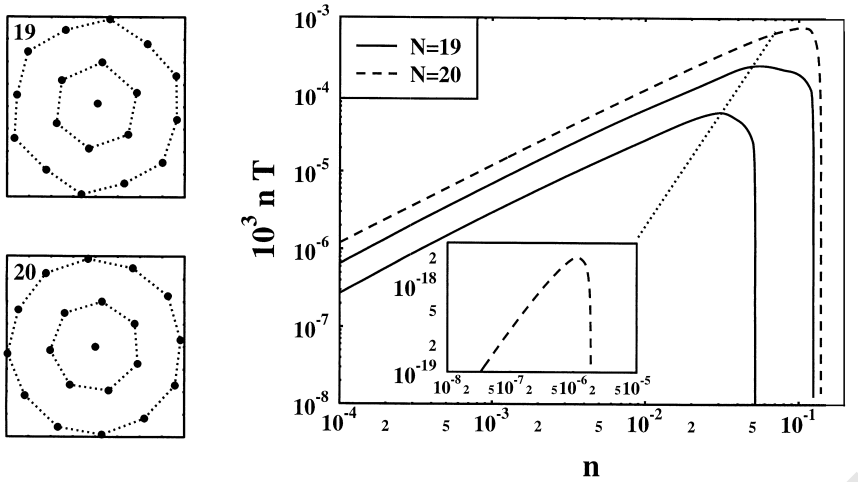

Fig. 1. Left two figures: Ground state configuration of the 'magic' cluster $N = 19$ (top) and $N = 20$ (bottom) in the cluster plane. Each dot is an electron. Right figure: Phase diagram of the Wigner crystal of 2D clusters with $N = 19$ and $N = 20$ electrons. The outer (inner) lines are the radial (angular) melting phase boundaries. The dotted diagonal line separates the classical (left) from the quantum (right) crystal. The classical part of the boundaries is given by lines with constant Γ, with the values (from top to bottom) $\Gamma_{20}^{\mathrm{RM}} = 83$, $\Gamma_{19}^{\mathrm{RM}} = 154$, $\Gamma_{19}^{\mathrm{OM}} = 330$ and $\Gamma_{20}^{\mathrm{OM}} = 3.4 \cdot 10^{11}$. The dimensionless density and temperature are given by $n = r_s^{-1/2}$ and $T \equiv 1/\Gamma$.

show a clear hexagonal crystal structure (Fig. 1, left part). In contrast, non-magic ones (e.g. $N = 20$) are dominated by the spherical trap symmetry. This has a strong effect on the stability of the crystal phases, see Fig. 1, right part.

Generally, crystal-like behavior[1] is found below a critical temperature (of the order of a few K in semiconductor quantum dots) in a finite density interval, see Fig. 1. If the density is reduced below a critical value $n_1(T,N)$, the system undergoes a transition to a state resembling a classical liquid. Similarly, above a second critical density $n_2(T,N)$ (with $n_2 \geq n_1$) a Fermi liquid-like state (in mesoscopic systems, sometimes referred to as Wigner molecule) is reached. While this general behavior is analogous to macroscopic systems, e.g. [5] crystallization in *few-electron* systems shows a number of interesting peculiarities[2]: (i) strong N dependence of the phase boundary, and (ii) the existence of a second phase boundary which is embedded into the first one where the crystal structure is transformed from a completely ordered ('OO', fully localized electrons) state into a partially ('RO', radially) ordered one where electrons are rigidly confined to crystal shells which, as a whole, can rotate against each other. The phase boundary is determined by critical values of the coupling parameters: the low-density boundary by the classical parameter, $\Gamma \equiv e^2/(\epsilon_b r_0 k_B T)$, and the high-density limit by $r_s \equiv r_0/a_B$, cf. Fig. 1. Here, a_B is the effective Bohr radius, $a_B = \hbar^2 \epsilon_b/(me^2)$, and r_0 is the mean interparticle distance, approximately given by the balance of the repulsive Coulomb force and the radial confinement force of the harmonic potential with strength ω_0: $e^2/(\epsilon_b r_0^2) = m\omega_0^2 r_0$. A

[1] We use the notations 'crystal', 'melting' and 'phase transition' to underline the analogy to the corresponding phenomena in infinite systems.

[2] In the simulations, the total spin has been fixed. Investigations on the spin properties of the ground state and of crystallization of mesoscopic clusters are presently under way.

particularly strong N dependence is observed for the 'OO' phase: 'magic' clusters ($N = 12,19$, etc.) are found to be much more stable than clusters having one electron more or less [2,3]. For example, the orientational melting parameters $\Gamma^{\rm OM}$ and $r_s^{\rm OM}$ of the cluster with $N = 19$ are *9 orders of magnitude* lower than those for $N = 20$, see Fig. 1.

This behavior can be exploited for a non-traditional control of crystallization. In addition to changing temperature or/and density (confinement strength), crystallization in mesoscopic systems can be achieved by variation of the particle number *without change of T and n*. For example, choosing a point in the temperature–density plane, Fig. 1, which is located between the radial (orientational) melting curves of $N = 19$ and $N = 20$ and switching between the two particle numbers is equivalent to a crossover between crystal-like and liquid-like (OO and RO crystal) behavior. We will demonstrate this below for the orientational melting curves in the classical part of the phase diagram, i.e. we fix the classical coupling parameter Γ between $\Gamma_{20}^{\rm OM}$ and $\Gamma_{19}^{\rm OM}$, (see Fig. 1, right part). The main difference between the orientationally ordered (with $N = 19$) and disordered ($N = 20$) state will be that the latter is able to support inter-shell rotational excitations. This should give rise to macroscopic currents and magnetic fields. To estimate this effect, we compute the total angular current created by N electrons confined to one of M shells of radius R_k rotating with angular frequency ω_k (positive or negative depending on the direction), $I_\phi = e\ \Sigma_{k=1}^{M}\ N_k\ \omega_k R_k$. The associated magnetic field on the symmetry axis in a distance z above the cluster plane is directed normal to the plane: $B_z(z,t) = \mu\ e/2\ \Sigma_{k=1}^{M}\ N_k\ \omega_k(t)[1+(z/R_k)^2]^{-3/2}$. For example, for $N = 20$, we have $N_1 = 7$, $N_2 = 12$, $R_2 \approx 2R_1 \approx 2\cdot r_0$, so that $I_\phi^{20} \approx e r_0(7\cdot\omega_1 + 24\cdot\omega_2)$. The relation between ω_1 and ω_2 depends on the excitation conditions. For example, if the total angular momentum of the excitation is zero, one readily finds $\omega_1/\omega_2 \approx -4N_2/N_1$, i.e. the inner shell rotates approximately seven times faster. Alternatively, rotation of some shells may be inhibited due to defects (pinning). For definiteness, in the following we consider the cluster $N = 20$ with the outer shell pinned.

At a given coupling Γ and confinement energy $m\omega_0 r_0^2/2$, thermal fluctuations spontaneously excite rotational and vibrational degrees of freedom both, in radial and angular direction. The thermal energy per particle is $k_{\rm B}T$ and is Γ times smaller than the confinement energy. As our simulations show (see below), approximately half of it is converted into angular kinetic energy (rotations and oscillations), i.e. $E_{\rm rot} \approx 1/4 m\omega_0^2 R_1^2/\Gamma$. Depending on the excitation conditions, this gives rise to rotations of the inner shell electrons with $\omega_{1\,\max} \approx \omega_0/\sqrt{2\Gamma}$. Inserting this result into the expression for B_z and averaging over the fast vibrations, we obtain

$$\langle B_z(z)\rangle_{\max} \approx \frac{\mu\, e^2}{2\epsilon_{\rm b} r_0}\,\frac{N_1}{\sqrt{m\, r_0 \Gamma}}\,[1+(z/r_0)^2]^{-3/2}.$$

Interestingly, the current and the magnetic field increase as the square root of temperature. In contrast, the cluster of 19 electrons does not support intershell rotations. Here, the excitation energy is completely converted into vibrations.

We have verified this concept by performing classical molecular dynamics simulations for $N = 19$ and $N = 20$ in a wide range of Γ values[3] [6]. As expected, the cluster with $N = 19$ (pinned to suppress the trivial rotation of the whole system) supports, at $\Gamma = 500 > \Gamma_{19}^{\rm OM}$, no intershell rotations, and only vibrations are excited, even for purely rotational initial fluctuations. In contrast, for $N = 20$, strong

[3] Animated simulation examples can be viewed at the web page http://elde.mpg.uni-rostock.de/mb

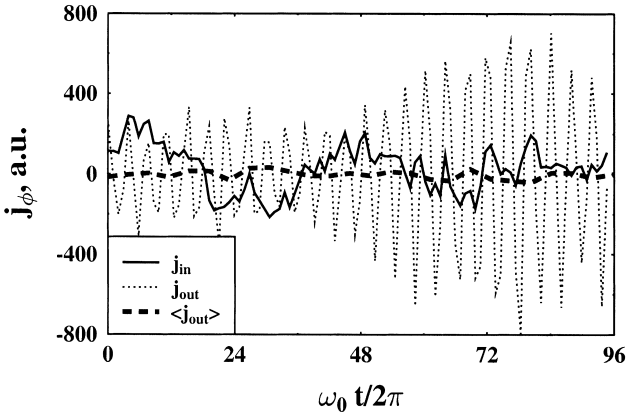

Fig. 2. Spontaneously excited angular currents of the inner ('in') and outer ('out') shell of an $N = 20$ cluster at $\Gamma = 500 \ll \Gamma_{20}^{OM}$ averaged over $T_0 = 2\pi/\omega_0$. The outer shell is pinned. The thick dashed line is j_{out} averaged over $4T_0$.

collective rotational motion of the inner shell electrons is excited, see Fig. 2. In all cases, we found that, in the spectrum, the vibrational excitations are well separated from the rotations—the former occur at significantly higher frequency, dominantly at frequency ω_0 (and $\omega_0/4$). After averaging over $4T_0$, with $T_0 = 2\pi/\omega_0$, a 'persistent' collective current $\langle j_{in} \rangle$ of the inner shell is observed which exceeds the averaged fluctuating signal $\langle j_{out} \rangle$ of the pinned outer shell by at least two orders of magnitude. The direction of the shell rotation and its slow time-dependence of $\langle j_{in} \rangle$ are determined by the (random) excitation conditions and is not relevant. As an independent test we computed the potential barriers for intershell rotation using Quantum Monte Carlo simulations [3]. These simulations effectively average over the random excitations and yield, for $N = 20$ at $\Gamma = 500$, potential barriers which are practically zero.

For practical applications, one may think of *designing* a suitable *external* rotational excitation in such a way that it is sufficiently weak so it does not overcome the barrier of the $N = 19$ cluster. If applied to the $N = 20$ cluster, the same excitation will easily give rise to intershell rotations. Such an excitation could be, e.g. a constant or pulsed circularly polarized electric field. Based on our simulations, we expect that the response of a (pinned) $N = 20$ cluster will be a nearly dissipationless rotation of the inner shell which stops after removal of one electron. This allows for a completely new kind of single-electron controlled devices. Such collective rotations of a group of electrons can be easily transmitted, e.g. in a system of multiple layers [7] and may find applications for quantum computing. Naturally, realization of this concept will require very clean samples, and detection of the weak circular currents is another important issue to be solved. At the same time, high sensitivity of these few-electron clusters to very weak rotational excitations could be of interest for applications by itself.

Acknowledgements

M.B. acknowledges stimulating discussions with participants of NPMS-5, in particular, J. Barker on quantum computing and K. von Klitzing on experimental verification issues. This work has been

139 supported by the Deutsche Forschungsgemeinschaft (Grant BO-1366/2) and by a grant for CPU time
140 at the NIC Jülich.

141 References

142 [1] R.C. Ashoori, Nature (London) 379 (1996) 413.
143 [2] V.M. Bedanov, F.M. Peeters, Phys. Rev. B 49 (1994) 2667.
144 [3] A.V. Filinov, M. Bonitz, Yu.E. Lozovik, Phys. Rev. Lett. 86 (2001) 3851.
145 [4] A.V. Filinov, Yu.E. Lozovik, M. Bonitz, Phys. Stat. Sol. (b) 221 (2000) 231.
146 [5] B. Tanatar, D.M. Ceperley, Phys. Rev. B 39 (1989) 5005.
147 [6] For the general simulation scheme, see V. Golubnychiy, M. Bonitz, D. Kremp, M. Schlanges, Phys. Rev. E 64 (2001)
148 016409.
149 [7] A. Filinov, M. Bonitz, Yu.E. Lozovik, Contrib. Plasma Phys. 41 (2001) 357.